Intuitive-augmented human-machine multidimensional nano-manipulation terminal using triboelectric stretchable strip sensors based on minimalist design

Tao Chen[a, b, c, #], Qiongfeng Shi[b, c, d, #], Minglu Zhu[b, c, d, e], Tianyiyi He[b, c, d, e], Zhan Yang[a, *], Huicong Liu[a, *], Lining Sun[a], Lei Yang[f] and Chengkuo Lee[b, c, d, e, *]

[a]Jiangsu Provincial Key Laboratory of Advanced Robotics, School of Mechanical and Electric Engineering & Collaborative Innovation Center of Suzhou Nano Science and Technology, Soochow University, Suzhou, P.R. China 215123
[b]Department of Electrical and Computer Engineering, National University of Singapore, 4 Engineering Drive 3, Singapore 117576
[c]Center for Intelligent Sensors and MEMS, National University of Singapore, E6 #05-11F, 5 Engineering Drive 1, Singapore 117608
[d]Hybrid-Integrated Flexible (Stretchable) Electronic Systems Program, National University of Singapore, E6 #05-4, 5 Engineering Drive 1, Singapore 117608
[e]NUS Suzhou Research Institute (NUSRI), Suzhou Industrial Park, Suzhou, China 215123
[f]Orthopaedic Insititute and Department of Orthopaedics, Soochow University, Suzhou, P.R. China 215006
#These authors contributed equally to this work.
* Email: yangzhan@suda.edu.cn; hcliu078@suda.edu.cn; elelc@nus.edu.sg

Supporting Information

Contents

Supporting Information 1: Fabrication of the strip.

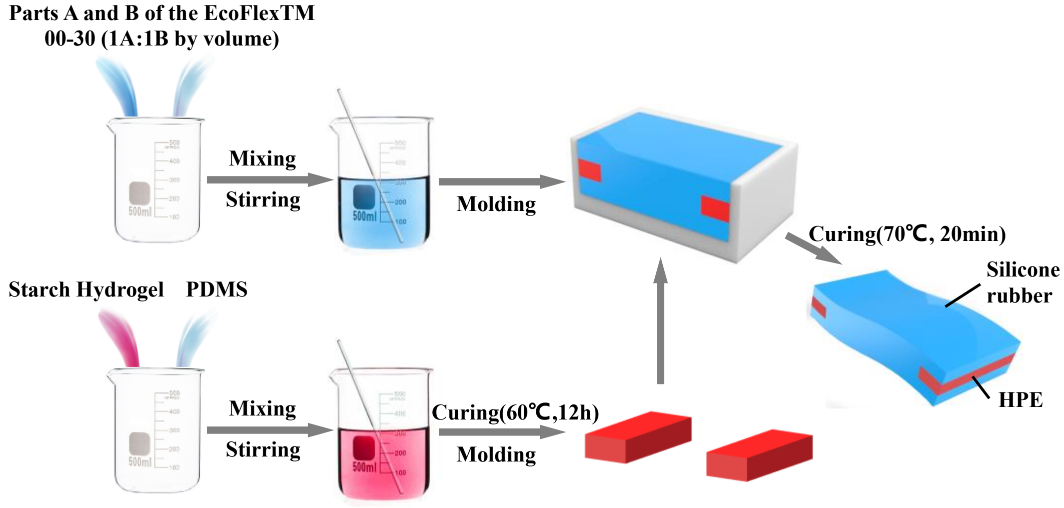

Figure S1. Fabrication of carbohydrate-based elastomer: Liquid PDMS was prepared by a mixing silicone elastomer base and cross-linker (Sylgard 184, Dow Corning) at a mass ratio of 10:1. Both starch-based hydrogel and liquid PDMS were degassed in a vacuum chamber to removing gas bubbles in the gel. Then they were mixed together at a volume ratio of 3:1 to obtain the precursor of Carbohydrate-based Elastomer. To remove the bubbles in the precursor, the precursor was centrifuged for 10 min at a speed of 3000 rpm.

Fabrication of silicone rubber and electrodes: After dispensing required amounts of Parts A and B of the EcoFlexTM 00-30 into a mixing container (1A:1B by volume), the blend was mixed thoroughly for 3 minutes and poured into the mold for thin film casting followed by a 20-minute baking at 70 ºC for curing. The HPE was placed at the corresponding position to form the electrode before the solution solidifies, and the position of HPE is fixed through an external wire until the solution solidifies.

Supporting Information 2. The strip and electrostatic analysis of the contact process.

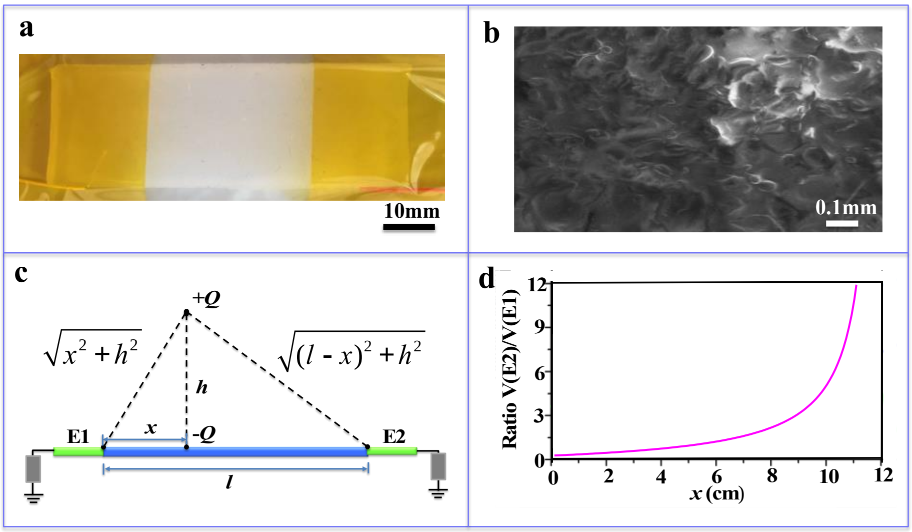

Figure S2. Photographs of strip and electrostatic analysis of the contact process. **a** The photograph of the strip. **b** The scanning electron microscopy (SEM) images of the silicone rubber structure. **d** The theoretical analysis curve corresponding to **c**.

Theoretical analysis of analogy method of the strip:

If the electric potential of ground and infinite distance is assumed to be of 0 V, then the electric potential of a point charge can be written as

$$U = k\frac{Q}{r} \tag{S1}$$

where Q is the amount of charge, r is the distance to the point charge and k is the Coulomb's constant.

The distance between two opposite electrodes (E1 and E2) is assumed to be l. After contact with the silicone rubber surface, the finger with a charge of $+Q$ moves away from the silicone rubber surface with a distance of h. The touch point on silicone rubber surface is with a charge of $-Q$ correspondingly. If the distance between the touch point and E1 is x, then the distance between the touch point and E2 is l-x. Thus, the electric potentials of the E1 and E2 (V_{E1} and V_{E2}) can be expressed as

$$\begin{cases} V_{E1} = k\frac{Q}{\sqrt{x^2+h^2}} - k\frac{Q}{x} \\ V_{E2} = k\frac{Q}{\sqrt{(l-x)^2+h^2}} - k\frac{Q}{l-x} \end{cases} \tag{S2}$$

Their ratio can be derived as

$$\frac{V_{E2}}{V_{E1}} = \frac{k\frac{Q}{\sqrt{(l-x)^2+h^2}}-k\frac{Q}{l-x}}{k\frac{Q}{\sqrt{x^2+h^2}}-k\frac{Q}{x}} = \frac{\frac{1}{\sqrt{(l-x)^2+h^2}}-\frac{1}{l-x}}{\frac{1}{\sqrt{x^2+h^2}}-\frac{1}{x}} \tag{S3}$$

Supporting Information 3. The dimensions of the TSS device.

Table S1. Dimensions of the device

Parameter Name	Value
Diameter of basement	150 mm
Thickness of basement	8 mm
Diameter of mobile stage	70 mm
Thickness of mobile stage	8 mm
Diameter of area limit	90 mm
height of height limit	38 mm
Length of strip pre-tensioned	40 mm

Supporting Information 4. The electrical characteristics of HPE.

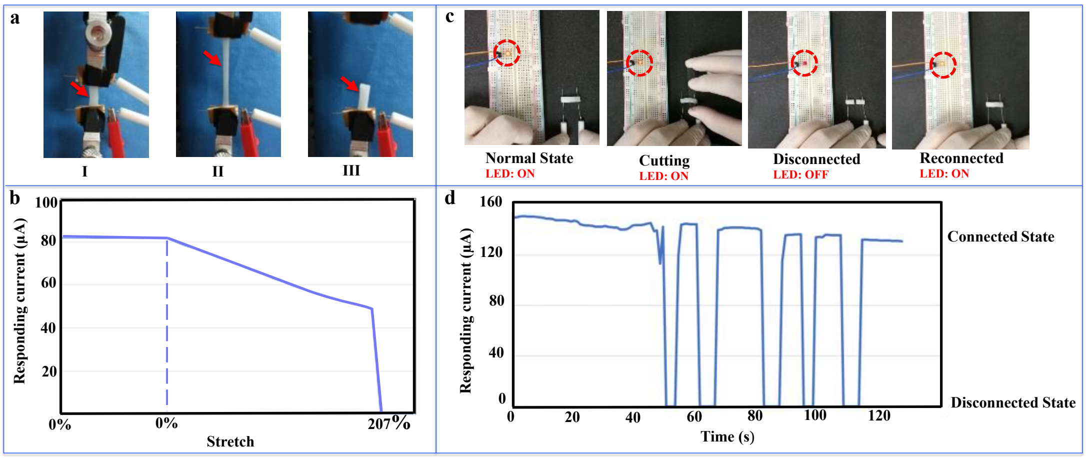

Figure S3. **a** Photographs of stretching test of HPE and **b** electrical characteristics curve under voltage of 1.5V. **c** The current curve of HPE disconnection and connection process in the circuit. **d** Electrical conductivity test of HPE. A piece of HPE is applied with a 3 V voltage at both ends.

Supporting Information 5. The reliability test of the strip.

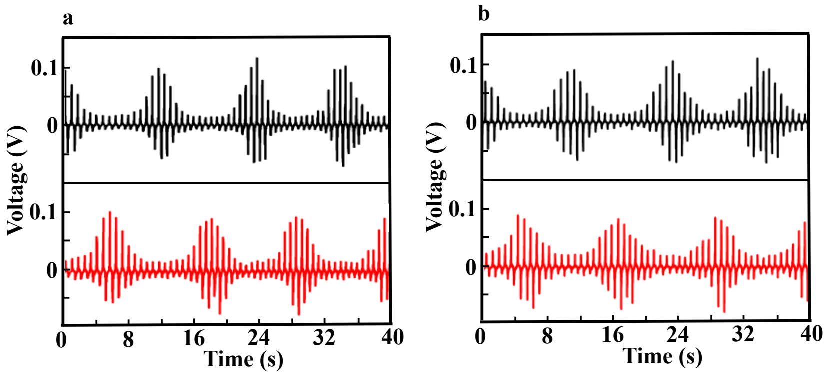

Figure S4. Reliability test of the strip for 10000 times stretching by linear motor. The finger knocks the strip reciprocally between the two electrodes, recording the corresponding signal characteristic curve before the stretchable test (**a**) and after the test (**b**).

Supporting Information 6. Theoretical analysis of the motion range of mobile stage in plane.

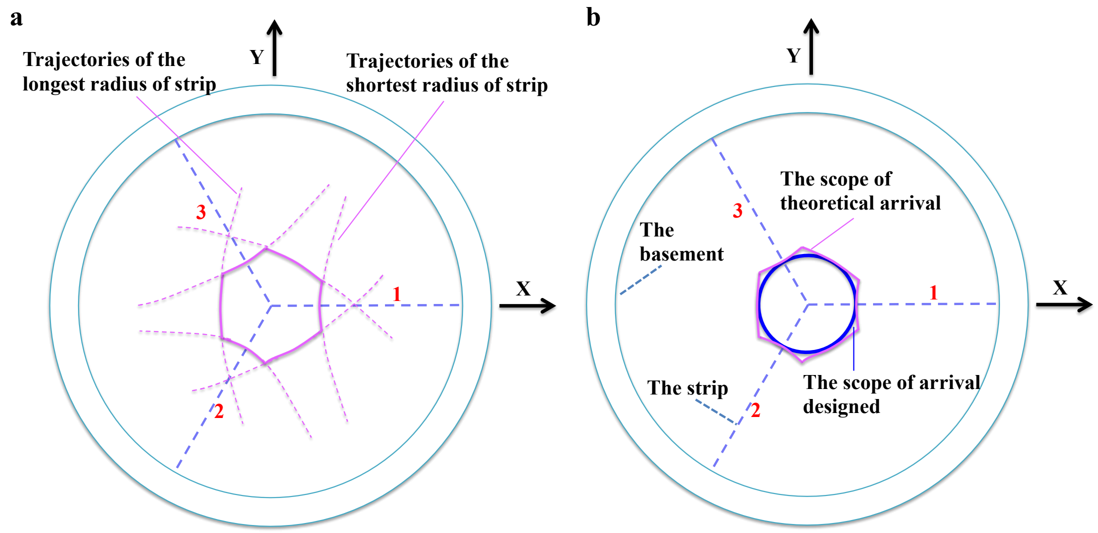

Figure S5. The strips are assembled in the device with 10 mm pre-tension length and the maximum stretch of each strip is set as 20 mm. Then, we draw the arc trajectory of the shortest radius and longest radius of the three strips respectively, and there will be a pink hexagonal overlaping region of the three strips as shown in **a**. That is the region of stage motion in plane. To facilitate the computation and control of motion, we draw the approximate region, as shown in the blue circle region in **b**. According to the circular area, the physical limitations are designed in the basement.

Supporting Information 7. Analysis of the relationship between the length of three strips and the motion displacement of the mobile stage along the five axes (X, Y, Z, α, β).

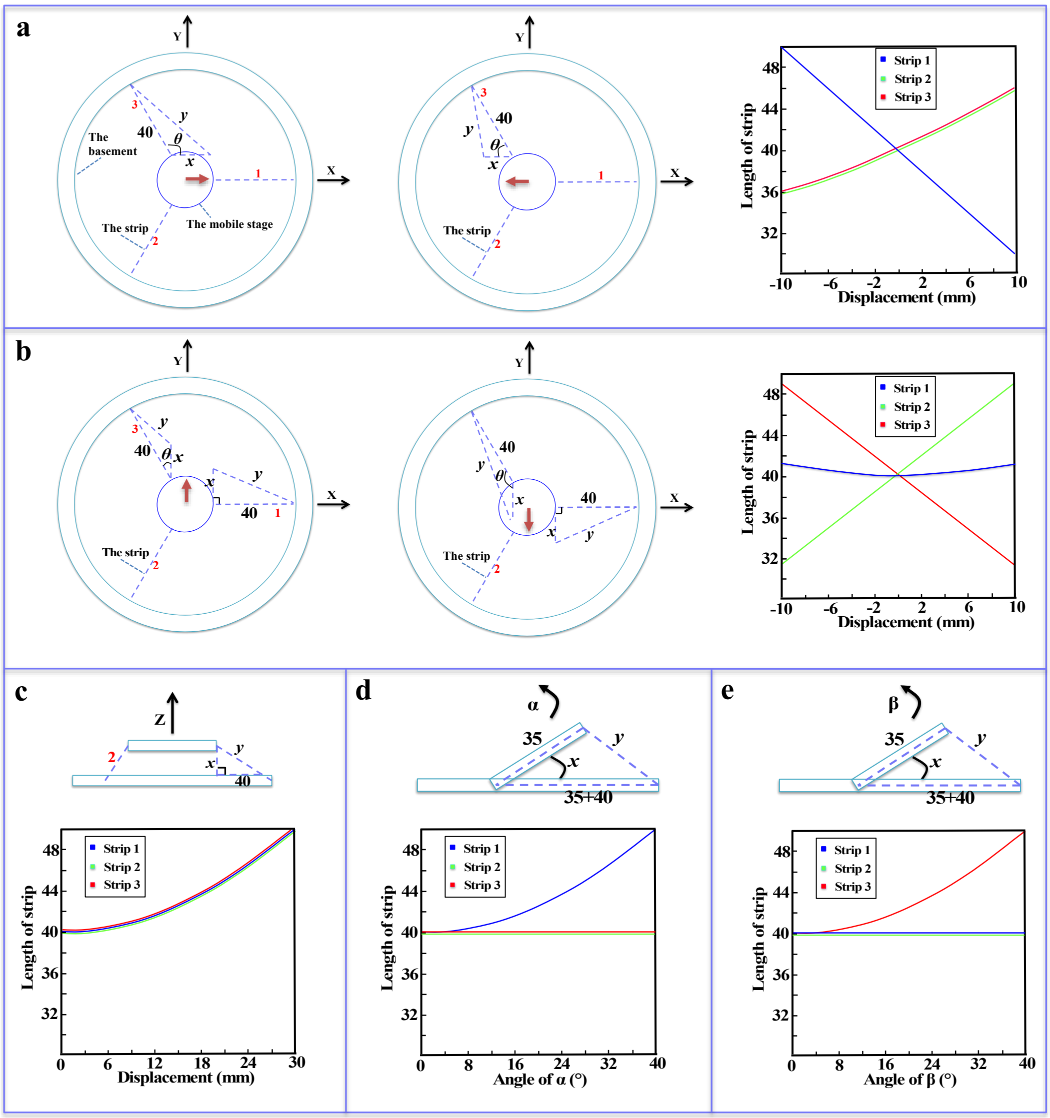

Figure S6. Analysis of the relationship between the length of three strips and the motion displacement of the mobile stage along the five axes (X, Y, Z, α, β).

The length of the three strips is 40 mm in the initial state, and center of stage is defined as origin of coordinates. When the stage moves along the X direction, the motion along the X axis is supposed to be "*x*" and the length of the strip is supposed to be "*y*". Then the relation between "*y*" and "*x*" can be derived by the cosine theorem:

$$y^2 = 40^2 + x^2 - 2 \cdot 40x \cdot cos\theta$$

The relation curve is shown in the Figure S5a. The strip 2 and strip 3 are symmetrical to the X axis, so two curves are the same trend. The length of strip 1 is linear along the X axis. The angle θ is 120° and 60° respectively in the direction of X and -X.

When the stage moves along the Y direction, the length change of strip 3 is also derived by cosine theorem. The strip 2 and strip 3 are symmetrical. The length change of strip 1 is derived through the relations of the edges of the right triangle. The relation curve is shown in the Figure S5b.

When the stage moves along the Z direction, the length changes of three strips are the same. They can be derived through the relations of the edges of the right triangle. The relation curve is shown in the Figure S5c.

The length of the lifting part of the stage is 35 mm when it rotates. Therefore, according to the cosine theorem, we calculate the relationship between the length of the strips and the angle as shown in the Figure S5d and e.

Supporting Information 8. The angular resolution of the device in XY plane.

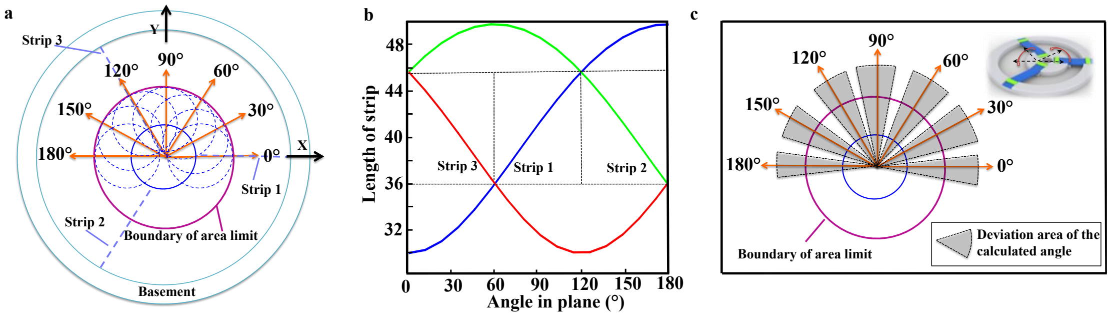

Figure S7. Angular resolution measurement in various directions of motion in XY plane. **a** Repetitive tests of the stage in different motion directions from 0 to 180 °, increasing in units of 30 °. **b** The variations of the strips length are calculated by cosine theorem when the stage moves along the area limit boundary from 0 to 180°. **c** The deviation angle of each measurement angle is drawn from the calculated angle values. At every 30 °, the deviation areas can be clearly distinguished without overlaping area at each measuring point. Therefore, the angle detection in XY plane has achieved a resolution of 30 °.

Supporting Information 9. Schematic diagram of electrical control connection.

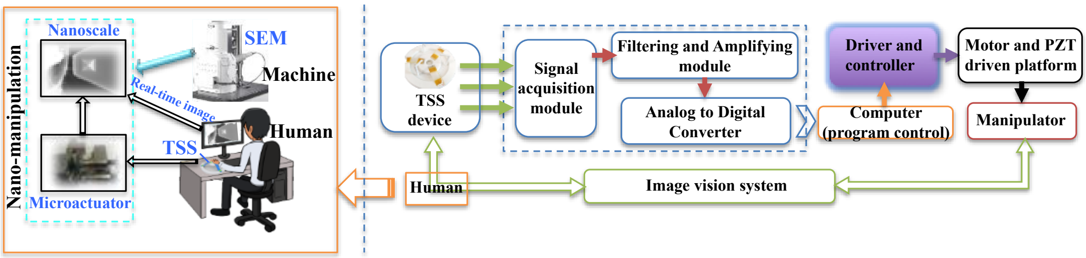

Figure S8. The TSS control terminal connects and communicates with the computer through the acquisition card and converter, then the control of the motor is realized through the controller. Finally, the operation of the manipulator is completed. The closed loop feedback of the whole system is realized by the image vision system.

Supporting Information 10. Schematic diagram of absolute coordinate and relative coordinate control method.

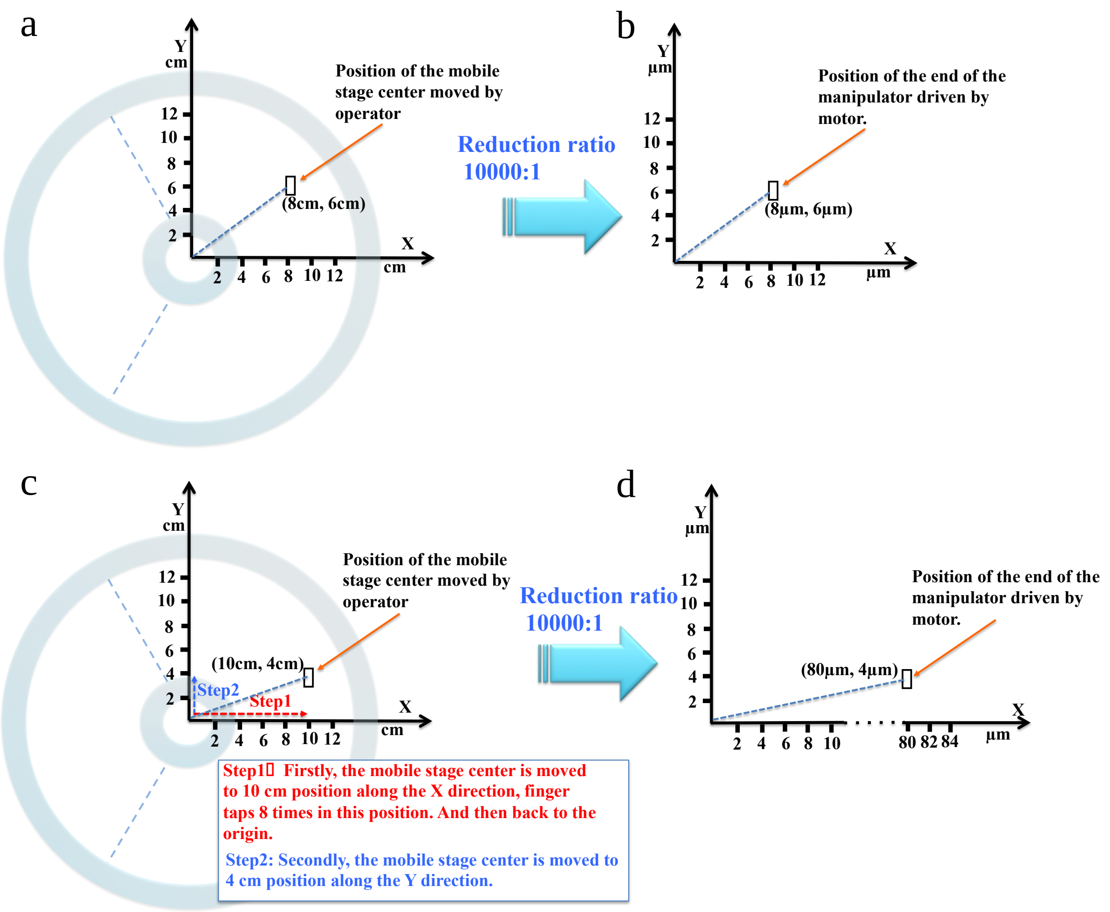

Figure S9. **a-b** Schematics of absolute coordinate control method. In this coordinate system, the motion direction of the end of manipulator matches to that of the mobile stage center, but with the ratio of 10000:1 in terms of displacement distance. **c-d** Schematic diagram of relative coordinate control method. In this coordinate system, the long-distance motion of the manipulator can be realized by multiple tapping to repeat the same motions further, which is not affected by the motion range stopper of the mobile stage. And hence, by controlling the motion length along two axes individually, the end of manipulator can move to any point in practical operation.

Supporting Information 11. The demonstrations of the TSS device to control the manipulator in SEM.

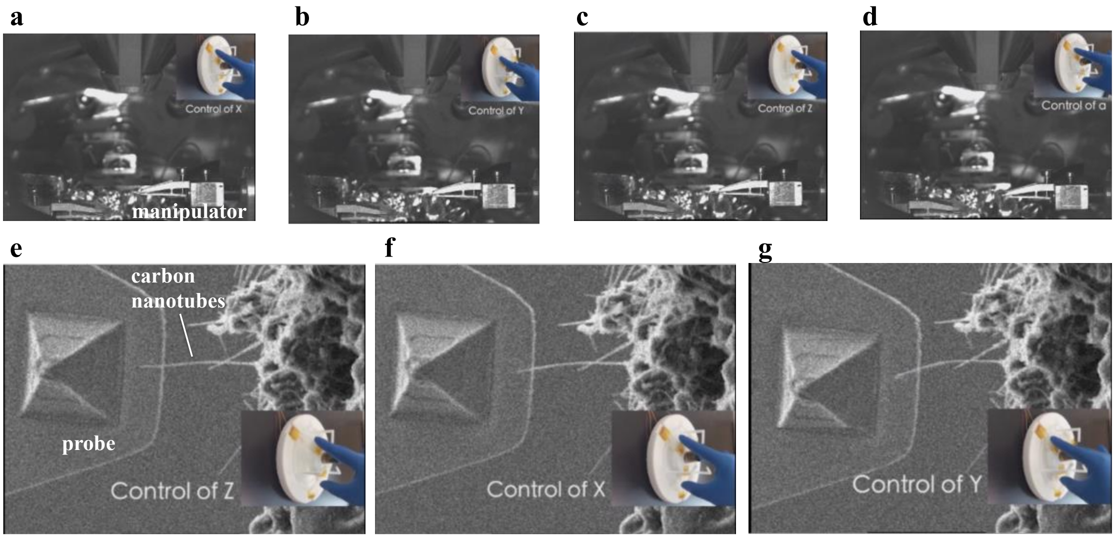

Figure S10. **a-d** The manipulator is controlled by the TSS device to carry out large-travel, multidimensional motion in macro scale. **e-g** The probe at the end of the manipulator realizes the operation of carbon nanotubes using the TSS control terminal.